



## OPEN ACCESS

## EDITED BY

José María Ponce-Ortega,  
Michoacana University of San Nicolás de  
Hidalgo, Mexico

## REVIEWED BY

Hongfei Liu,  
PetroChina Planning and Engineering Institute,  
China  
Heriberto Alcocer-García,  
Michoacana University of San Nicolás de  
Hidalgo, Mexico

## \*CORRESPONDENCE

Andrey Goluntsov,  
✉ gas.ru@mail.ru

RECEIVED 03 November 2025

REVISED 06 January 2026

ACCEPTED 06 January 2026

PUBLISHED 27 January 2026

## CITATION

Nikolaev A, Goluntsov A and Plotnikova K (2026)  
A physically based rheological model for  
predicting the flow behavior of non-newtonian  
crude oil mixtures under cold  
climate conditions.  
*Front. Chem. Eng.* 8:1736520.  
doi: 10.3389/fceng.2026.1736520

## COPYRIGHT

© 2026 Nikolaev, Goluntsov and Plotnikova.  
This is an open-access article distributed under  
the terms of the [Creative Commons Attribution  
License \(CC BY\)](https://creativecommons.org/licenses/by/4.0/). The use, distribution or  
reproduction in other forums is permitted,  
provided the original author(s) and the copyright  
owner(s) are credited and that the original  
publication in this journal is cited, in accordance  
with accepted academic practice. No use,  
distribution or reproduction is permitted which  
does not comply with these terms.

# A physically based rheological model for predicting the flow behavior of non-newtonian crude oil mixtures under cold climate conditions

Alexander Nikolaev, Andrey Goluntsov\* and Kristina Plotnikova

Department of Oil and Gas Transportation and Storage, Saint-Petersburg Mining University, Saint Petersburg, Russia

Accurate prediction of the rheological behavior of heavy crude oil mixtures is essential for pipeline transport under cold climate conditions. This study presents a physically based non-Newtonian rheological model that incorporates the coupled effects of temperature and mixture composition through temperature- and concentration-dependent expressions for the consistency coefficient and flow behavior index. The model was calibrated and validated using 88 experimental rheological measurements on binary mixtures of heavy Severo-Komsomolskoye and light Vankor crudes over a temperature range of 5C–60 °C, heavy-oil concentrations of 0%–100%, and shear rates of 1–300 s<sup>-1</sup>. The proposed model predicts shear stress with a mean relative deviation of 8.7% and a root mean square error below 0.95 Pa, outperforming conventional Arrhenius, Refutas, and classical power-law correlations by a factor of 2–3. The model accurately captures the transition from non-Newtonian to near-Newtonian behavior with increasing temperature and dilution, providing a practical tool for hydraulic calculations and flow assurance design in cold-region pipeline systems.

## KEYWORDS

cold climate conditions, flow assurance, heavy oil mixtures, non-Newtonian crude oil, pipeline transport, rheological modeling, temperature-dependent viscosity

## 1 Introduction

The transportation of heavy and non-Newtonian crude oils in cold regions has become a pressing global issue due to the rising importance of unconventional oil resources and the depletion of lighter crude reserves (Shammazov et al., 2025; Pshenin et al., 2025; Skorobogatov et al., 2025; Litvinen et al., 2020). Heavy and extra-heavy crudes are characterized by high viscosity and complex flow behavior, which severely limit their mobility. In cold climates, these difficulties are intensified, as low ambient temperatures increase viscosity, promote wax and asphaltene precipitation, and heighten the risk of flow blockages. These factors contribute to higher energy consumption, reduced operational reliability, and significant environmental and economic risks (Souas et al., 2020; Jing et al., 2023; Dvoynikov and Kutuzov, 2025; Lyu et al., 2019; Silva-Oliver et al., 2020). Ensuring reliable and energy-efficient transport of heavy crude oils is therefore critical for global energy security, particularly in regions where harsh climatic conditions prevail (Jing et al., 2023; Dvoynikov and Kutuzov, 2025; Lyu et al., 2019).

## 1.1 Problem statement and challenges

The key challenges in heavy crude oil pipeline transport are associated with the accurate prediction of rheological properties, hydraulic resistance, and flow assurance strategies. Heavy oils typically exhibit pronounced non-Newtonian behavior, including shear-thinning and yield-stress effects, making conventional viscosity correlations inadequate for describing flow under dynamic temperature and compositional conditions (Souas et al., 2020; Falconi et al., 2018; Saleh et al., 2021; Robidas and Gogoi, 2020). Hydraulic resistance is another major concern: the high viscosity of these oils causes significant frictional losses, requiring increased pumping capacity and leading to elevated operational costs (Souas et al., 2020; Jing et al., 2023; Saleh et al., 2021). Moreover, in cold climates, precipitation of waxes and asphaltenes further complicates flow, threatening pipeline integrity and necessitating advanced flow assurance measures (Jing et al., 2023; Lyu et al., 2019).

## 1.2 Literature review: existing rheological models

A variety of viscosity and rheological models have been proposed for crude oil transport, yet most face significant limitations when applied to heavy oils. Arrhenius- and Refutas-type models are widely used for temperature–viscosity relationships but are often unable to account for non-Newtonian effects in oil mixtures (Robidas and Gogoi, 2020; Jing et al., 2020). Bingham and Herschel–Bulkley models are useful for fluids with yield stress but may fail to capture the full complexity of heavy oil rheology under varying dilution and thermal conditions (Falconi et al., 2018; Saleh et al., 2021; Hoshyargar and Ashrafzadeh, 2013). Similarly, Koval and power-law models have been applied to emulsions and multiphase systems, but their predictive power decreases at extreme shear rates and compositions (Saleh et al., 2021; Hoshyargar and Ashrafzadeh, 2013; Pilehvari et al., 1988). Finally, empirical correlations are often developed for light and medium crudes, making them unsuitable for predicting flow behavior of heavy and non-Newtonian oils, particularly under cold conditions (Silva-Oliver et al., 2020; Robidas and Gogoi, 2020; Jing et al., 2020). These shortcomings highlight the need for more comprehensive approaches that integrate temperature, concentration, and molecular interaction effects.

The study of changes in the rheological properties of non-Newtonian crude oils during blending represents a challenging task, since crude oil is a multicomponent fluid with a highly diverse chemical composition.

Additive models traditionally applied to petroleum systems do not always provide sufficiently accurate predictions of property variations in mixtures containing non-Newtonian crude oils. This limitation often leads to increased pumping costs and reduced energy efficiency of pipeline transportation.

Non-Newtonian crude oil is a hydrocarbon fluid whose rheological behavior deviates from the classical Newtonian law, exhibiting effective viscosity dependence not only on temperature  $T$  and pressure  $P$ , but also on shear rate  $\dot{\gamma}$ , deformation time  $t$ , and

shear stress  $\tau$ . Thus, in a generalized form, the effective viscosity may be expressed as Equation 1:

$$\eta = f(T, P, \dot{\gamma}, t, \tau). \quad (1)$$

To predict the viscosity of binary crude oil mixtures, a variety of mathematical models have been developed. Table 1 summarizes the most widely used formulations, including both theoretical and empirical approaches. These models can be broadly classified into three groups according to their underlying principles and degree of empirical adjustment.

The Arrhenius, Bingham, Koval, and Kendall–Monroe models are grounded in physical principles that assume ideal or simplified mixing of components. While mathematically straightforward and computationally efficient, they fail to capture the complexity of real systems. In particular, they neglect intermolecular interactions, structural effects, and molecular associations. As a result, these models are inadequate when the component viscosities differ significantly, since they cannot describe the nonlinear effects observed in real crude oil mixtures or account for density and temperature influences.

The Wallace–Henry, Al-Basrah, Chevron, Shan–Peng (No. 1 and No. 2), and Walther models extend theoretical constructs—typically involving logarithmic or mean-value relationships—by incorporating empirical correction terms or employing transformed equations calibrated against experimental data. Compared with purely theoretical models, they offer improved predictive accuracy by considering the influence of fluid density, interaction mechanisms, and correction coefficients. However, their use is generally restricted to specific types of crude oils or mixtures for which they were originally developed.

Finally, the Cragoe, Maxwell, Refutas, Parkash, and Latour/Miadonye models are entirely empirical in nature, derived from large sets of experimental measurements. They are often expressed as complex exponential or double-logarithmic functions obtained through regression analysis. These models can successfully reproduce viscosity behavior across a wide range of crude oils and blending ratios, making them particularly suitable for engineering calculations. Nevertheless, their application requires precise input parameters and a relatively high degree of computational accuracy.

In general, these mathematical models describe mixture viscosity as a function of the viscosities of the constituent components, while neglecting the influence of temperature, pressure, and shear rate variations.

## 1.3 Recent advances (brief)

To overcome the limitations of conventional models, recent research has introduced new approaches that integrate both theoretical developments and practical engineering solutions. Temperature- and dilution-dependent viscosity models have improved prediction accuracy for transport limits and phase inversion points in oil mixtures (Silva-Oliver et al., 2020; Jing et al., 2020). Complementary to this, computational fluid dynamics (CFD) and artificial intelligence (AI) techniques are increasingly used to simulate complex non-Newtonian flow

TABLE 1 Mathematical models for predicting the viscosity of binary crude oil mixtures (Al-Maamari et al., 2015).

Model name	Equation	Type	Ref.
Arrhenius	$\ln(\nu_{mix}) = x_1 \ln(\nu_1) + x_2 \ln(\nu_2)$	Theoretical	Riazi (2005)
Bingham	$\nu_{mix}^{-1} = x_1 \nu_1^{-1} + x_2 \nu_2^{-1}$	Theoretical	Mehrotra et al. (1996)
Cragoe	$\nu_{mix} = 0,0005 \cdot \exp\left(\frac{1000 \ln(20)}{I_{Cr}}\right)$	Theoretical	Cragoe (1929)
	$I_{Cr} = x_1 I_{Cr1} + x_2 I_{Cr2}$		
	$I_{Cr i} = \frac{1000 \ln(20)}{\ln\left(\frac{\nu_i}{0,0005}\right)}$		
Maxwell	$\nu_{mix} = \exp\left(\exp\left(\frac{I_M - 59,58959}{-21,8373}\right)\right) - 0,8$	Theoretical	Maxwell (1972)
	$I_M = x_1 I_{M1} + x_2 I_{M2}$		
	$I_{Mi} = 59,58959 - 21,8373 \cdot \ln(\ln(\nu_i + 0,8))$		
Koval	$\nu_{mix}^{-0,25} = x_1 \nu_1^{-0,25} + x_2 \nu_2^{-0,25}$	Empirical	Koval (1963)
Wallace and henry	$\nu_{mix} = 0,01 \exp\left(\frac{1}{I_{WH}}\right)$	Empirical	Wallace and Henry (1955)
	$I_{WH} = x_1 I_{WH1} + x_2 I_{WH2}$		
	$I_{WH i} = \frac{1}{\ln\left(\frac{\nu_i}{0,01}\right)}$		
Al-basrah	$\ln(\nu_{mix}) = x_1 \ln(\nu_1) + x_2 \ln(\nu_2) - 4,976 \cdot 10^{-3} \cdot x_1 x_2 (API_1 - API_2)^2$	Empirical	Al-Basrah (2004)
Refutas	$\nu_{mix} = \exp\left(\exp\left(\frac{I_R - 10,975}{14,534}\right)\right) - 0,8$	Empirical	Refutas (1991)
	$I_R = x_1 I_{R1} + x_2 I_{R2}$		
	$I_{Ri} = 10,975 + 14,534 \cdot \ln(\ln(\nu_i + 0,93425))$		
Latour/Miadonye	$\nu_{mix} = \exp\left(\exp\left(\alpha(1 - x_2^n) + \ln(\nu_2) - 1\right)\right)$	Empirical	Miadonye et al. (2000)
	$\alpha = \ln(\ln(\nu_1) - \ln(\nu_2) + 1)n = \frac{\nu_2}{0,09029 \nu_2 + 0,1351}$		
Parkash	$\nu_{mix} = \exp\left(\exp\left(\frac{I_P - 10,975}{14,534}\right)\right) - 0,93425$	Empirical	Parkash (2003)
	$I_P = x_1 I_{P1} + x_2 I_{P2}$		
	$I_{Pi} = -157,43 + 376,38 \cdot \ln(\ln(\nu_i + 0,93425))$		
Chevron	$\nu_{mix} = 10^{\frac{3I_C}{1-I_C}}$	Empirical	Chevron Research Company (1979)
	$I_C = x_1 I_{C1} + x_2 I_{C2}$		
	$I_{Ci} = \frac{\ln(\nu_i)}{3 + \ln(\nu_i)}$		
Shan-peng no. 1	$\lg(\lg(\nu_{mix})) = x_1 \lg(\lg(\nu_1)) + x_2 \lg(\lg(\nu_2)) + C_{12} x_1 x_2$	Empirical	Shan and Peng (2004)
	$C_{12} = -0,0613 \cdot (\lg(\nu_1) + \lg(\nu_2)) + 0,134$		
Shan-peng no. 2	$\lg(\lg(\nu_{mix})) = x_1 \lg(\lg(\nu_1)) + x_2 \lg(\lg(\nu_2)) + C_{12} x_1 x_2$	Empirical	Kendall and Monroe (1917)
	$C_{12} = -0,0644 \cdot (\lg(\nu_1) + \lg(\nu_2)) + 0,1706$		
Kendall and monroe	$\nu_{mix}^{\frac{1}{3}} = x_1 \nu_1^{\frac{1}{3}} + x_2 \nu_2^{\frac{1}{3}}$	Empirical	Walter (1951)
Walther	$\lg(\lg(\nu_{mix} + 0,6)) =$	Empirical	Gudala et al. (2020)
	$= x_1 \lg(\lg(\nu_1 + 0,6)) + x_2 \lg(\lg(\nu_2 + 0,6))$		

behaviors and optimize pipeline design and operation (Saleh et al., 2021; Jing et al., 2020; Al-Maamari et al., 2015).

On the applied side, chemical and mechanical innovations have demonstrated considerable potential to enhance flow assurance and reduce energy consumption. The development of biodegradable additives, advanced surfactants, and stable oil-in-water emulsions has shown the ability to significantly reduce viscosity, enabling stable transport even under subzero temperatures (Al-Maamari et al.,

2015; Rushd et al., 2023). Simultaneously, advances in drag-reduction strategies—including biomimetic surface treatments, novel drag-reducing agents, and boundary layer control methods—contribute to minimizing hydraulic losses and enhancing throughput (Rushd et al., 2023; Kumar and Mahto, 2017).

Thermal management technologies are another area of progress. Emulsification techniques combined with advanced thermal insulation, such as photothermal coatings, help maintain flow

stability and lower heating requirements in cold climates (Jing et al., 2020; Lyu et al., 2019). These solutions not only address technical challenges but also support sustainable pipeline operations by reducing environmental impact and energy demand (Lyu et al., 2019; Al-Maamari et al., 2015).

## 1.4 Research gap and contributions

Overall, recent advances reflect a shift toward integrated strategies that combine rheological modeling, computational methods, chemical treatments, and thermal technologies. Their application in industry demonstrates that modern heavy oil transportation research is increasingly focused on balancing operational efficiency, cost-effectiveness, and environmental responsibility.

Despite the wide range of viscosity and rheological models proposed for crude oil mixtures, several fundamental limitations remain unresolved when these models are applied to non-Newtonian heavy oils under cold climate conditions. Most existing correlations account for either temperature effects or compositional variation, but rarely address their coupled influence on non-Newtonian flow behavior. In particular, classical Arrhenius- and Refutas-type models neglect shear-dependent effects altogether, while conventional power-law and Herschel–Bulkley formulations typically assume constant rheological parameters, which is physically inconsistent for systems undergoing thermal and compositional changes.

Furthermore, commonly used mixing rules implicitly assume ideal or near-ideal blending behavior and therefore fail to capture nonlinear inter-component interactions, especially in mixtures exhibiting abrupt rheological transitions associated with asphaltene aggregation and paraffin crystallization at low temperatures. As a result, these models often lose predictive accuracy under cold climate conditions and at high heavy-oil concentrations, precisely where reliable rheological prediction is most critical for flow assurance.

The present work addresses these limitations by proposing a physically based rheological model in which both the consistency coefficient and the flow behavior index are expressed as explicit functions of temperature and mixture composition, augmented by interaction parameters that account for nonlinear structural effects. Unlike conventional approaches, the proposed formulation enables continuous prediction of rheological behavior across wide temperature and concentration ranges while preserving correct limiting behavior for pure components. This provides a unified framework for predicting non-Newtonian flow behavior of crude oil mixtures under cold climate conditions.

The main contributions of this study are threefold:

1. Development of a rheological model that simultaneously accounts for temperature, composition, and non-Newtonian effects in crude oil mixtures.
2. Introduction of inter-component interaction parameters that capture nonlinear and abrupt rheological transitions observed experimentally.
3. Experimental validation of the proposed model over a wide range of temperatures, concentrations, and shear rates relevant to cold-region pipeline operation.

## 2 Methodology

### 2.1 Model development workflow

The proposed rheological model was developed following a stepwise methodology that integrates physical reasoning, experimental observations, and empirical parameter identification. As a starting point, the Ostwald–de Waele (power-law) model was selected as the base formulation due to its widespread use in describing shear-thinning behavior of non-Newtonian crude oils. However, in contrast to classical implementations with constant rheological parameters, the present approach assumes that both the consistency coefficient and the flow behavior index vary systematically with temperature and mixture composition.

In the first stage, temperature effects were incorporated by introducing exponential temperature-dependent expressions for the consistency coefficient and the flow behavior index. This reflects the physical weakening of intermolecular interactions, including asphaltene and paraffin associations, with increasing temperature. In the second stage, concentration effects were introduced by expressing these rheological parameters as functions of the heavy crude oil fraction in the mixture. To account for non-ideal blending behavior, inter-component interaction terms were included, enabling the model to capture nonlinear and asymmetric effects observed during dilution.

In the final stage, additional correction parameters were introduced to describe experimentally observed abrupt rheological transitions occurring at low temperatures and high heavy-oil concentrations. These parameters represent concentration-induced structural instabilities and allow the model to reproduce sharp changes in viscosity and shear stress that cannot be captured by smooth interpolation alone. The resulting formulation provides a unified expression for shear stress and apparent viscosity as simultaneous functions of temperature, composition, and shear rate.

### 2.2 Experimental program

The experimental component of the methodology was designed to provide comprehensive rheological data for model calibration and validation. Binary mixtures of high-viscosity Severo-Komsomolskoye crude oil and low-viscosity Vankor crude oil were prepared over a wide range of volumetric ratios, covering the full composition interval from pure light to pure heavy crude. Rheological measurements were performed using a rotational rheometer under controlled thermal conditions.

Experiments were conducted over a temperature range of 5 °C–60 °C and shear rates from 1 to 300 s<sup>-1</sup>, corresponding to operating conditions relevant to pipeline transport in cold regions. A full factorial multi-level experimental design was employed to systematically investigate the combined influence of temperature and mixture composition. Detailed descriptions of materials, sample preparation, measurement procedures, and experimental design are provided in the Materials and Methods section.

## 2.3 Parameter estimation and validation

Model parameters were identified through systematic processing of the experimental data. For each temperature and mixture composition, shear stress–shear rate data were analyzed in logarithmic coordinates to determine the consistency coefficient and flow behavior index from linear regression. These experimentally derived parameters formed the basis for subsequent calibration of the temperature- and concentration-dependent model functions.

Empirical coefficients governing temperature dependence, concentration effects, and inter-component interactions were determined by minimizing the deviation between experimentally measured and model-predicted shear stress values over the entire dataset. To evaluate predictive robustness and avoid overfitting, the experimental data were divided into calibration and validation subsets, with approximately 70% of the data used for parameter estimation and 30% reserved for independent validation.

Model performance was assessed using statistical error metrics, including the mean relative deviation and root mean square error. The resulting calibrated model was then used to predict shear stress and viscosity across the full range of investigated temperatures, compositions, and shear rates, enabling direct comparison with experimental observations in the Results and Discussion section.

## 2.4 Applicability range and limitations

The proposed rheological model is applicable within the range of conditions covered by the experimental program, namely temperatures from 5 °C to 60 °C, heavy crude oil concentrations from 0% to 100%, and shear rates between 1 and 300 s<sup>-1</sup>. The model is formulated for steady-state shear flow and was calibrated using laboratory-scale rheological measurements. Outside this range, particularly at temperatures below 5 °C or under transient and viscoelastic flow conditions, additional structural effects may arise that are not explicitly accounted for in the present formulation. Therefore, extrapolation beyond the validated domain should be performed with caution.

## 3 Theoretical model

The derivation of the proposed rheological model follows a stepwise approach: first, temperature effects on the consistency coefficient and flow index are considered; second, concentration effects and inter-component interactions are introduced; finally, correction terms are incorporated to capture experimentally observed abrupt transitions.

The dependence of the dynamic viscosity coefficient on temperature is commonly expressed by the Arrhenius (Equation 2)

$$\mu = \mu_0 \cdot e^{AT} \quad (2)$$

where  $\mu$  is the dynamic viscosity (mPa·s),  $\mu_0$  is the initial viscosity (mPa·s),  $A$  is a constant, and  $T$  is the temperature.

One of the most widely applied rheological models is the Ostwald–de Waele power-law mode

$$\tau = K\dot{\gamma}^n \quad (3)$$

where the consistency coefficient  $K$  characterizes the viscosity, and the flow index  $n$  characterizes the degree of non-Newtonian behavior. Both parameters depend on temperature and on the properties of the fluid under study, and thus on the concentration of components in the mixture (Equations 4, 5):

$$K = K(T, C); \quad (4)$$

$$n = n(T, C). \quad (5)$$

Taking the logarithm of Equation 3, we obtain Equation 6

$$\ln(\tau) = \ln(K) + n \cdot \ln(\dot{\gamma}) \quad (6)$$

or, more explicitly,

$$\ln(\tau) = \ln(K(T, C)) + n(T, C) \cdot \ln(\dot{\gamma}). \quad (7)$$

Equation 7 has the form of a linear regression, in which the parameters depend on both temperature and concentration. To clarify this dependence, let us consider how the consistency coefficient  $K$  and the flow index  $n$  vary with temperature  $T$  and the volume fraction of heavy crude in the mixture  $C$ .

The consistency coefficient  $K(T, C)$  reflects the internal structural stability of the fluid (Buslaev and Konoplyannikov, 2026). As temperature increases, molecular interactions weaken; therefore, viscosity and the consistency coefficient decrease. Empirical observations indicate that  $K$  decreases exponentially with increasing temperature (Equation 2):

$$K_i(T) = K_0 \cdot e^{AT} \quad (8)$$

This relation illustrates that increasing temperature reduces the strength of intermolecular associations (asphaltenes, resins, paraffins), thereby enhancing fluid mobility. In practical pipeline operation, this means that heating the crude reduces the pressure drop and lowers the pumping energy demand.

When non-Newtonian crude is blended with a diluent, the composition directly influences the consistency coefficient through changes in the mixture's structure. In the simplest case, if the components do not interact, their contributions to  $K$  are proportional to their concentrations, leading to a linear expression

$$K(C) = K_1(T) \cdot (1 - C) + K_2(T) \cdot C \quad (9)$$

Thus, each component contributes to the viscosity of the mixture in proportion to its fraction. In reality, however, interactions between components must be taken into account. To reflect this, Equation 9 is extended with interaction terms

$$K(T, C) = (K_1(T) \cdot (1 - C))^{\beta_{K1}} + (K_2(T) \cdot C)^{\beta_{K2}} \quad (10)$$

where  $\beta_{K1}$  and  $\beta_{K2}$  are inter-component interaction coefficients.

The dependence of  $K$  on concentration demonstrates that a diluent not only reduces viscosity but also interacts with the heavy crude fraction. The symmetry or asymmetry of the interaction coefficients reflects the sensitivity of the mixture: in some cases, even small additions of diluent drastically reduce viscosity ("thinning effect"), whereas in others the effect is negligible. From an operational perspective, selecting the optimal crude-to-diluent ratio can substantially reduce pumping costs.

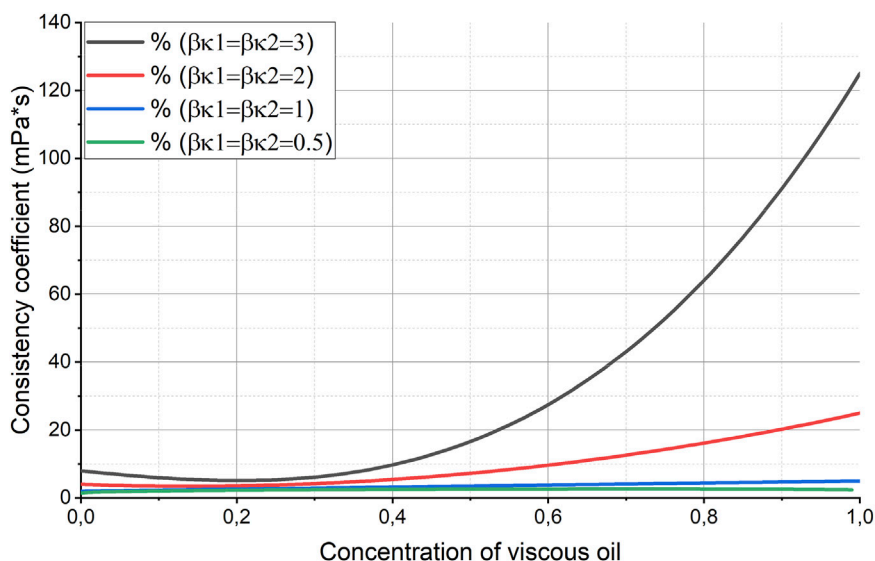


FIGURE 1 Dependence of the consistency coefficient on the concentration of viscous oil in the mixture at symmetric values of the intercomponent interaction coefficients  $\beta_{K1}$  and  $\beta_{K2}$ .

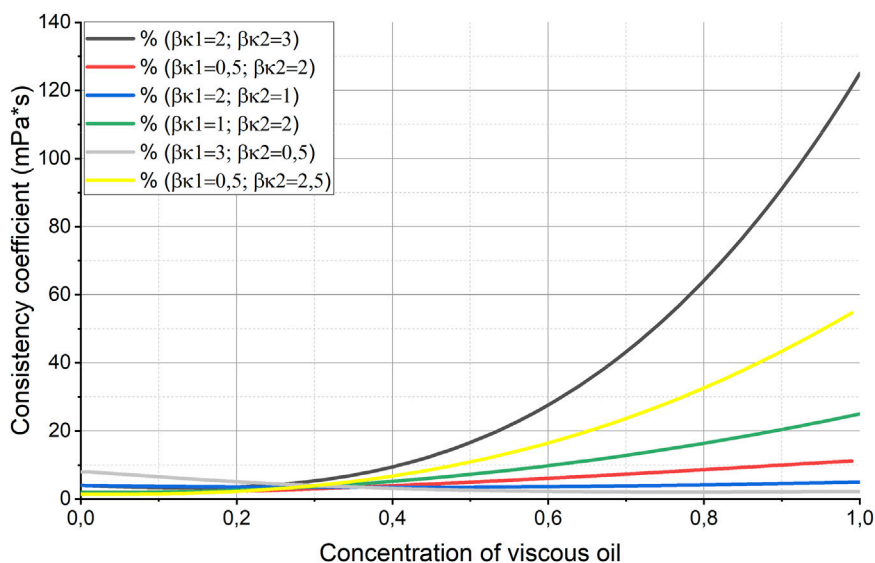


FIGURE 2 Dependence of the consistency coefficient on the concentration of viscous oil in the mixture at asymmetric values of the intercomponent interaction coefficients  $\beta_{K1}$  and  $\beta_{K2}$ .

The coefficients  $\beta_{K1}$  and  $\beta_{K2}$  account for nonlinear effects arising from physicochemical interactions between components. They are symmetric with respect to concentration substitution, reflecting the mutual contribution of both fluids. At the boundary conditions, when  $C = 0$

$$K(T, 0) = K_1(T)^{\beta_{K1}}$$

and when  $C = 1$

$$K(T, 1) = K_2(T)^{\beta_{K2}}$$

Thus, in the limiting cases of pure components, Equation 10 reduces to the temperature-dependent properties of a single crude oil.

If  $\beta_{K1} = \beta_{K2} = 1$ , the model becomes a linear weighted sum. In the case of  $\beta_{K1} = \beta_{K2} \neq 1$ , the dependence is symmetric (Figure 1). When  $\beta_{K_i} > 1$ , the contribution of the corresponding component is amplified, especially at higher concentrations; when  $\beta_{K_i} < 1$ , its influence diminishes even at high concentration. The condition  $\beta_{K1} \neq \beta_{K2}$  allows the model to capture asymmetric nonlinear interactions between mixture components (Figure 2).

The proposed model is physically consistent, correctly reflects the limiting states of the mixture, and is capable of describing the nonlinear influence of each component on the overall rheological properties.

Substituting the values of  $K_i(T)$  (Equation 8) for  $K_1(T)$  and  $K_2(T)$  into Equation 10, the consistency coefficient  $K(T, C)$  is given by

$$K(T, C) = ((K_{0,1} \cdot e^{A_1 T}) \cdot (1 - C))^{\beta_{K1}} + ((K_{0,2} \cdot e^{A_2 T}) \cdot C)^{\beta_{K2}} \quad (11)$$

Comparison with experimental data indicates that the model provides a smooth interpolation but does not account for anomalous variations in the consistency coefficient. To capture sharp changes in  $K(T, C)$  during the mixing of non-Newtonian fluids, it is proposed to use Equation 11 in the following modified form

$$K(T, C) = ((K_{0,1} \cdot e^{A_1 T}) \cdot (1 - C))^{\beta_{K1}} + ((K_{0,2} \cdot e^{A_2 T}) \cdot C)^{\beta_{K2}} + \alpha C \cdot (1 - C) \quad (12)$$

where  $\alpha$  is a coefficient accounting for potential sharp variations of the consistency coefficient during the mixing of non-Newtonian liquids.

Physically, the parameter  $\alpha$  represents the intensity of concentration-induced structural instability in the mixture. Higher values of  $\alpha$  correspond to systems in which small compositional changes lead to significant variations in the internal microstructure, resulting in sharp changes in apparent viscosity. Conversely,  $\alpha \rightarrow 0$  reduces Equation 12 to a smooth interpolation, corresponding to weak or negligible interaction effects.

The flow index characterizes the degree of deviation of the fluid properties from Newtonian behavior. Its dependence on temperature and component concentration is associated with changes in the microstructure of the fluid during mixing and heating. Upon heating, the thermal motion of molecules disrupts the structure (including asphaltenes and paraffins), bringing the fluid closer to Newtonian behavior. To describe this transition, the exponential approximation is employed

$$n_i(T) = 1 + (n_{i,0} - 1) \cdot e^{-k_i(T_2 - T_1)}, \quad (13)$$

where  $n_{i,0}$  is the value of  $n_i$  at temperature  $T_1$ ;

$k_i$  is the rate coefficient for the transition of the flow index  $n$  toward unity;  $T_1$  is the temperature at which the initial values  $n_{i,0}$  are determined;  $T_2$  is the temperature of the fluid under investigation.

The flow index quantifies the extent of non-Newtonian behavior. Heating causes the disruption of asphaltene and paraffin aggregates. Equation 13 is illustrated in Figure 3.

Let us consider the possible constraints for function (Equation 11). For  $T_1 = T_2$ , the equation reduces to Equation 14

$$n_i(T) = n_{i,0}. \quad (14)$$

For  $T_2 > T_1$ , the exponential term decays,  $e^{-k_i(T_2 - T_1)} \rightarrow 0$ , and  $n_i(T) \rightarrow 1$ . That is, with increasing temperature, the flow index approaches unity, indicating Newtonian behavior.

For  $T_2 < T_1$ , the exponential term increases. In this case, the model  $n(T)$  becomes invalid. Therefore, to use Equation 11, it is necessary to impose the restriction that the temperature at which the

initial parameter values are determined must be less than or equal to the temperature of the fluid under investigation  $T_2 \geq T_1$ .

The coefficient  $k_i$  must be strictly positive; if  $k_i < 0$ , the exponential term will grow, leading to  $n_i(T) \rightarrow \infty$  or  $n_i(T) \rightarrow -\infty$ .

Thus, the parameter constraints for the function  $n_i(T)$  (Equation 12) are system of Equation 15:

$$\begin{cases} T_2 \geq T_1 \\ k_i > 0 \end{cases}. \quad (15)$$

The influence of the mixture components concentration on the flow index follows the law of additivity. To account for physicochemical interactions between the components and the nonlinear effects of these processes, empirical coefficients must be introduced. Then, the dependence of the flow index on both temperature and component concentration can be expressed as

$$n(T, C) = n_1(T) \cdot (1 - C)^{\xi_1} + n_2(T) \cdot C^{\xi_2}, \quad (16)$$

where  $\xi_1$  and  $\xi_2$  are empirical coefficients that determine the degree of nonlinearity in the variation of the flow index with component concentration.

This equation indicates that not only temperature but also the concentration of the diluent affects the degree of non-Newtonian behavior. From an engineering perspective, this implies that the addition of a diluent can not only reduce viscosity but also make the oil more Newtonian, thereby reducing the risk of errors in pressure drop calculations and, consequently, hydraulic resistance.

Substituting  $n_i(T)$  from Equation 13 into Equation 16, and taking  $T_2 - T_1 = \Delta T$ , can be obtained

$$n(T, C) = \left(1 + (n_{1,0} - 1) \cdot e^{-k_1 \cdot \Delta T}\right) \cdot (1 - C)^{\xi_1} + \left(1 + (n_{2,0} - 1) \cdot e^{-k_2 \cdot \Delta T}\right) \cdot C^{\xi_2}. \quad (17)$$

Equation 17 describes the change in the flow index considering temperature variations during the mixing of non-Newtonian oil. Similarly to Equation 12, sharp changes in the flow index must also be accounted for

$$n(T, C) = \left(1 + (n_{1,0} - 1) \cdot e^{-k_1 \cdot \Delta T}\right) \cdot (1 - C)^{\xi_1} + \left(1 + (n_{2,0} - 1) \cdot e^{-k_2 \cdot \Delta T}\right) \cdot C^{\xi_2} + \beta C \cdot (1 - C), \quad (18)$$

where  $\beta$  is a coefficient accounting for possible abrupt changes in the flow index during the mixing of non-Newtonian fluids.

From a physical standpoint,  $\beta$  quantifies the sensitivity of the non-Newtonian character of the mixture to compositional perturbations. Larger values of  $\beta$  indicate a pronounced disruption of the dispersed asphaltene–paraffin structure, leading to a rapid increase of  $n$  toward unity.

Considering the obtained dependencies of the consistency coefficient (Equation 12) and the flow index (Equation 18), the Ostwald–de Waele power-law model (Equation 3) can be written as

$$\tau(T, C) = \left( ((K_{0,1} \cdot e^{A_1 T}) \cdot (1 - C))^{\beta_{K1}} + ((K_{0,2} \cdot e^{A_2 T}) \cdot C)^{\beta_{K2}} + \alpha C \cdot (1 - C) \right)$$

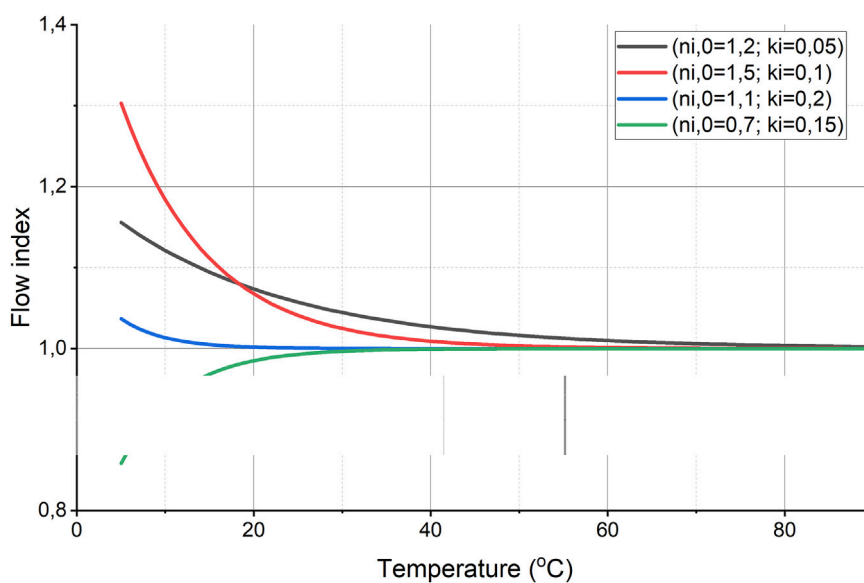


FIGURE 3 Dependence of the flow index on temperature for different values of  $n_{i,0}$  and  $k_i$ .

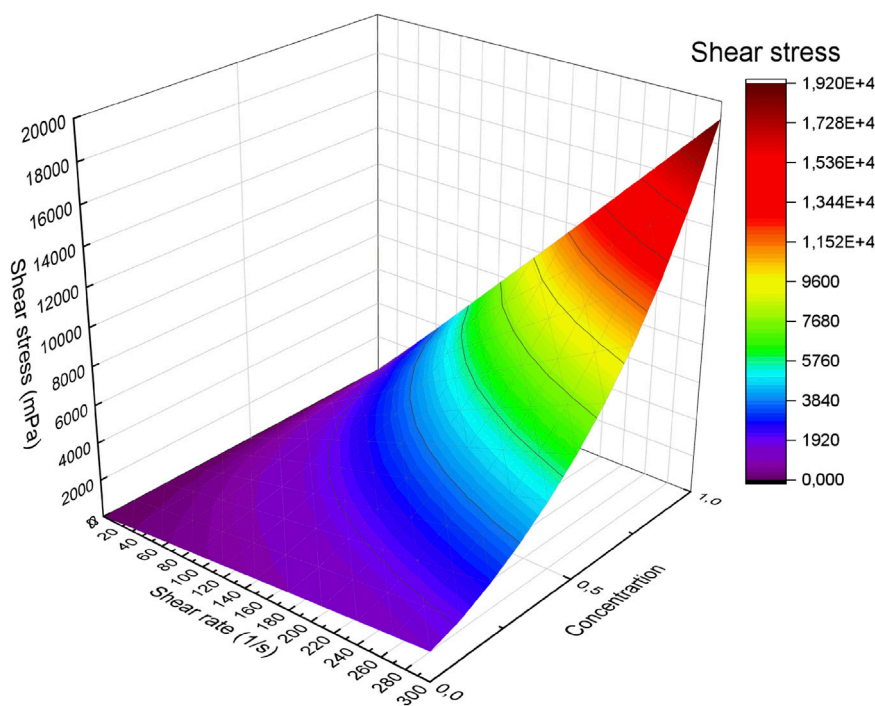


FIGURE 4 Dependence of shear stress on temperature and the concentration of highly viscous oil in the mixture according to Equation 19.

$$\times \dot{\gamma}^{(1+(n_{1,0}-1) \cdot e^{-k_1 \cdot \Delta T}) \cdot (1-C)^{\xi_1} + (1+(n_{2,0}-1) \cdot e^{-k_2 \cdot \Delta T}) \cdot C^{\xi_2} + \beta C \cdot (1-C)} \quad (19)$$

The graphical representation of this dependence is shown in Figure 4.

Similarly, the dynamic viscosity is expressed as

$$\eta(T, C) = \left( (K_{0,1} \cdot e^{A_1 T}) \cdot (1-C)^{\beta_{K1}} + ((K_{0,2} \cdot e^{A_2 T}) \cdot C)^{\beta_{K2}} + \alpha C \cdot (1-C) \right) \times \dot{\gamma}^{(1+(n_{1,0}-1) \cdot e^{-k_1 \cdot \Delta T}) \cdot (1-C)^{\xi_1} + (1+(n_{2,0}-1) \cdot e^{-k_2 \cdot \Delta T}) \cdot C^{\xi_2} + \beta C \cdot (1-C) - 1} \quad (20)$$

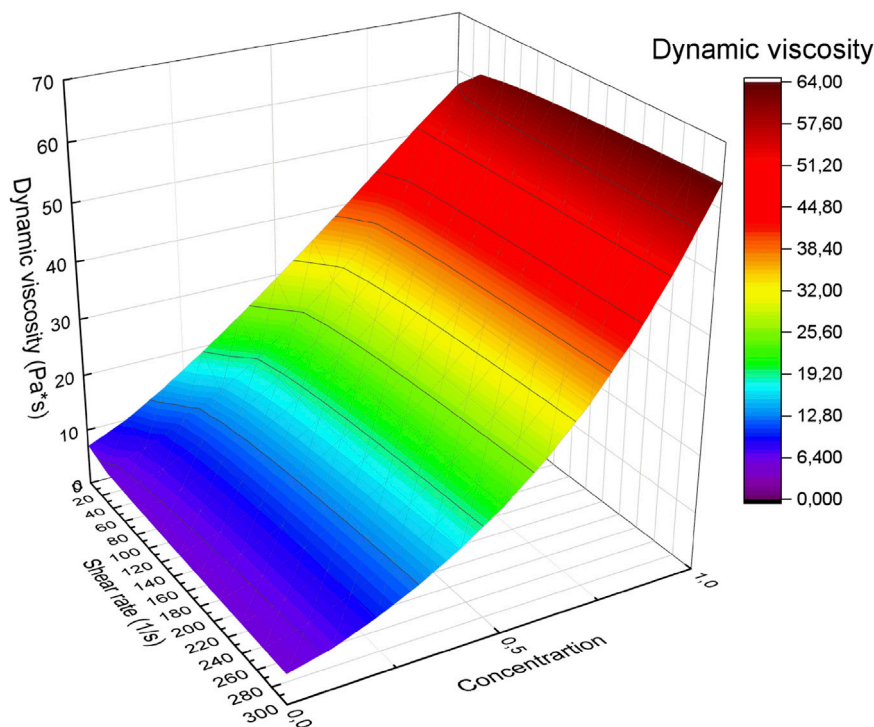


FIGURE 5  
Dependence of dynamic viscosity on temperature and the concentration of highly viscous oil in the mixture according to Equation 20.

Equations 19, 20 relate shear stress and dynamic viscosity simultaneously to temperature and component concentration. In other words, they allow laboratory data on mixture properties to be translated into real operational parameters. This enables the prediction of pressure at pumping stations based on soil temperature and mixture composition.

It is evident that the consistency coefficient and flow index functions must be determined empirically based on conducted experimental studies.

The graphical representation of the dependence described by Equation 19 is shown in Figure 5.

## 4 Materials and Methods

### 4.1 Experimental materials

The experimental investigation was carried out using crude high-viscosity oil samples obtained from the Severo-Komsomolskoye oil field and low-viscosity samples of the Vankor oil field (Figure 6). To ensure a comprehensive investigation of rheological behavior, binary mixtures of the Severo-Komsomolskoye (high-viscosity) and Vankor (low-viscosity) crudes were prepared in volumetric ratios of 1/9, 2/8, 3/7, 4/6, 5/5, 6/4, 7/3, 8/2, and 9/1. These proportions were selected to provide detailed coverage of the entire compositional range, allowing systematic evaluation of viscosity and shear-dependent flow properties across different blending ratios.

### 4.2 Rheological measurements

Rheological measurements were performed using a rotational rheometer Rheotest RN 4.1 (Figure 7), which allows precise determination of shear stress, shear rate, and viscosity under controlled thermal conditions. The instrument operates by measuring the torque required to rotate one cylindrical or conical element relative to another, providing direct evaluation of shear-dependent viscosity.

Experiments were conducted in a shear rate range of 1–300  $s^{-1}$  and a temperature range of 5 °C–60 °C, corresponding to expected operational conditions in northern pipeline systems. The measurement protocol included three stages (Figure 8):

- CR sweep (0  $\rightarrow$  300  $s^{-1}$ ), where the shear rate was gradually increased;
- CR constant (300  $s^{-1}$ ), where the sample was held at a constant shear rate;
- CR sweep (300  $\rightarrow$  0  $s^{-1}$ ), where the shear rate was decreased back to zero.

Prior to testing, samples were degassed, thermostabilized, and equilibrated for 15–20 min to ensure uniformity. Each test was repeated at least three times to ensure reproducibility.

### 4.3 Experimental design

A full factorial multi-level design was employed to systematically study the influence of two independent factors:



FIGURE 6  
Severo-Komsomolskoye and Vankor oil fields on map.

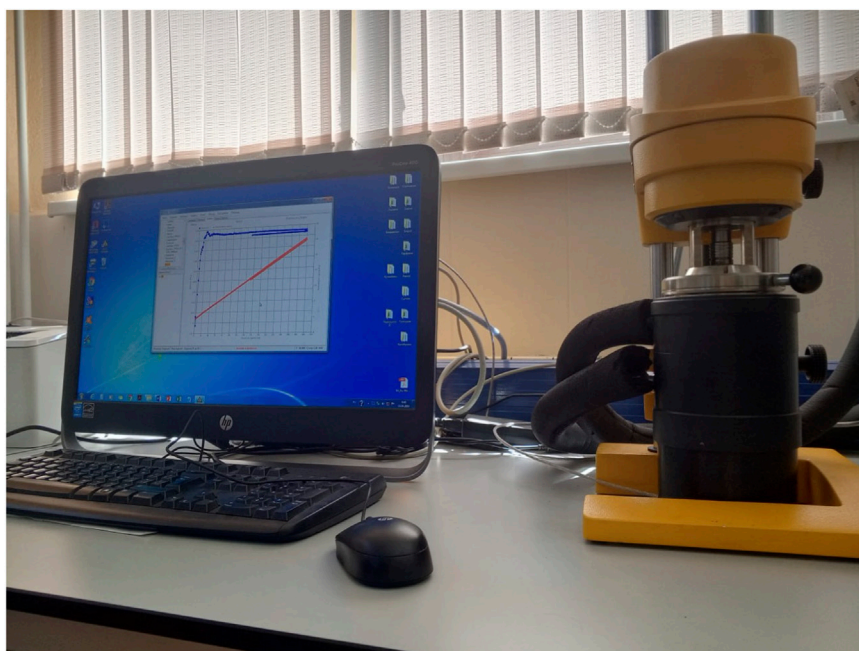


FIGURE 7  
Rheotest RN 4.1 viscometer.

Temperature ( $X_1$ ): 5 °C–60 °C;

Concentration of Severo-Komsomolskoye crude in mixture ( $X_2$ ): 0%–100%.

The experimental design was structured according to standard multifactorial planning methods (Huan et al., 2024; Jackson, 1994), including both two-level and three-level factorial designs, which were extended to a full multi-level matrix to improve accuracy. To this end, temperature and high-viscosity oil concentration factors were coded as shown in Table 2.

In total, 88 experimental runs were performed to cover the specified ranges of temperature and concentration (Table 3).

#### 4.4 Data processing and analysis

Shear stress ( $\tau$ ) and dynamic viscosity ( $\eta$ ) were determined for each experimental point using the relationship as Equation 21

$$\eta = \frac{\tau}{\dot{\gamma}} \quad (21)$$

where  $\dot{\gamma}$  is the applied shear rate.

Data were processed to eliminate measurement artifacts (e.g., local heating effects at high shear rates). Averaged results were used to construct flow curves  $\tau(\dot{\gamma})$  and viscosity curves  $\eta(\dot{\gamma})$  at different temperatures and mixture compositions. The results were further

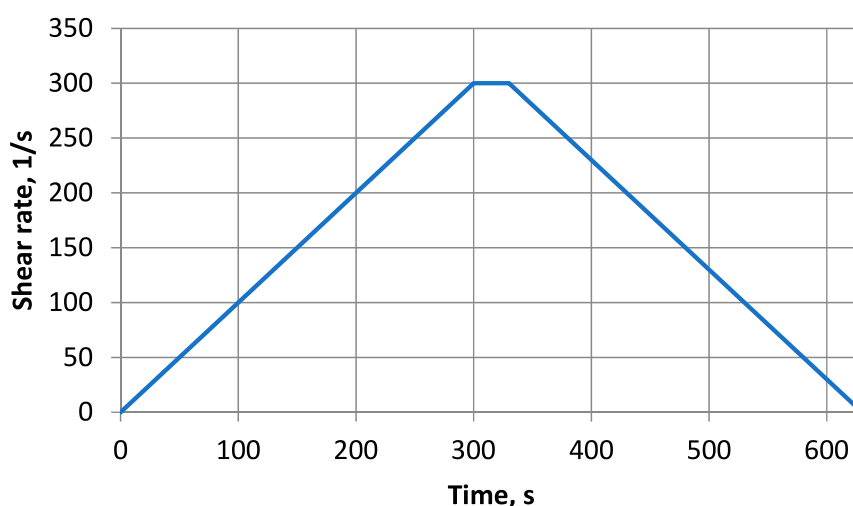


FIGURE 8  
Viscosimeter operating modes chart.

TABLE 2 Coding of factor levels.

Factor level	Temperature, °C	Concentration of heavy oil, %
1	5	0
2	10	10
3	15	20
4	20	30
5	30	40
6	40	50
7	50	60
8	60	70
9	—	80
10	—	90
11	—	100

analyzed to identify Newtonian and non-Newtonian regimes, yield stress behavior, and temperature–concentration effects.

The empirical parameters  $\alpha$  and  $\beta$  were calibrated simultaneously with the remaining model coefficients using the full experimental dataset (88 runs). Their values were selected to ensure accurate reproduction of experimentally observed inflection points and regions of rapid rheological transition, which could not be captured by conventional power-law formulations.

At the first stage of data processing, only the experimental points that were statistically significant and representative of steady-state flow conditions were selected for further analysis. All anomalous points associated with measurement fluctuations or instrument stabilization were excluded.

For each temperature and concentration, plots of the dependence

$$\ln(\tau) = \ln(K) + n \cdot \ln(\dot{\gamma})$$

were constructed. From the slope and intercept of these linear plots, the flow behavior index  $n$  and the consistency coefficient  $K$  were determined for each experimental condition.

Subsequently, the obtained  $K$  and  $n$  values were organized into tables showing their dependence on both temperature and concentration. Separate datasets were compiled for  $K(T)$ ,  $K(C)$ ,  $n(T)$ , and  $n(C)$ , which served as the basis for parameter estimation of the proposed model.

Initial approximate values of all empirical coefficients in the governing equations were then assigned. By iteratively adjusting these empirical parameters, the deviation between the experimentally determined and model-calculated values of the consistency coefficient  $K$  and the flow index  $n$  was minimized. The optimal set of parameters was obtained when the total mean-square deviation between predicted and experimental data reached its minimum, ensuring the best fit of the model to the experimental results.

TABLE 3 Plan-matrix of a complete multilevel two-factor experiment.

Exp no.	X1	X2	Exp no.	X1	X2	Exp no.	X1	X2	Exp no.	X1	X2
1	1	1	23	7	3	45	5	6	67	3	9
2	2	1	24	8	3	46	6	6	68	4	9
3	3	1	25	1	4	47	7	6	69	5	9
4	4	1	26	2	4	48	8	6	70	6	9
5	5	1	27	3	4	49	1	7	71	7	9
6	6	1	28	4	4	50	2	7	72	8	9
7	7	1	29	5	4	51	3	7	73	1	10
8	8	1	30	6	4	52	4	7	74	2	10
9	1	2	31	7	4	53	5	7	75	3	10
10	2	2	32	8	4	54	6	7	76	4	10
11	3	2	33	1	5	55	7	7	77	5	10
12	4	2	34	2	5	56	8	7	78	6	10
13	5	2	35	3	5	57	1	8	79	7	10
14	6	2	36	4	5	58	2	8	80	8	10
15	7	2	37	5	5	59	3	8	81	1	11
16	8	2	38	6	5	60	4	8	82	2	11
17	1	3	39	7	5	61	5	8	83	3	11
18	2	3	40	8	5	62	6	8	84	4	11
19	3	3	41	1	6	63	7	8	85	5	11
20	4	3	42	2	6	64	8	8	86	6	11
21	5	3	43	3	6	65	1	9	87	7	11
22	6	3	44	4	6	66	2	9	88	8	11

The empirical parameters of the proposed rheological model were determined using an iterative nonlinear regression procedure. As an objective function, the mean squared deviation between experimentally measured and model-predicted shear stress values was minimized over the calibration dataset as Equation 22

$$J = \frac{1}{N} \sum_{i=1}^N (\tau_i^{exp} - \tau_i^{calc})^2 \quad (22)$$

where  $N$  is the number of experimental data points. Initial parameter estimates were obtained from linear regressions of the logarithmic shear stress–shear rate data and from physically reasonable bounds inferred from the experimental trends. Model parameters were then updated iteratively to reduce the objective function value.

Convergence was assumed when the relative change in the objective function between successive iterations fell below  $10^{-6}$ , and when further parameter updates produced changes in the predicted shear stress smaller than the experimental uncertainty. The optimization process was additionally constrained to ensure physically meaningful parameter values, including positivity of the consistency coefficient and monotonic trends of rheological parameters with temperature. The final parameter set

corresponded to the global minimum of the objective function within the explored parameter space.

To assess the predictive robustness of the proposed model, the experimental dataset was partitioned into two subsets. Approximately 70% of the data were used for parameter calibration, while the remaining 30% served as an independent validation set. The partitioning was performed to ensure representative coverage of the full temperature and concentration ranges in both subsets.

The predictive accuracy obtained for the validation subset was comparable to that of the calibration data, indicating stable model behavior and the absence of overfitting.

## 5 Results and discussion

The experimental investigation of the rheological behavior of the Severo-Komsomolskoye (heavy) and Vankor (light) crude oils, as well as their binary mixtures, demonstrated distinct non-Newtonian characteristics for the heavy component and Newtonian behavior for the light one. The flow curves  $\tau(\dot{\gamma})$  obtained for the heavy crude revealed a pronounced shear-thinning effect, which diminished progressively with increasing temperature. In contrast, the

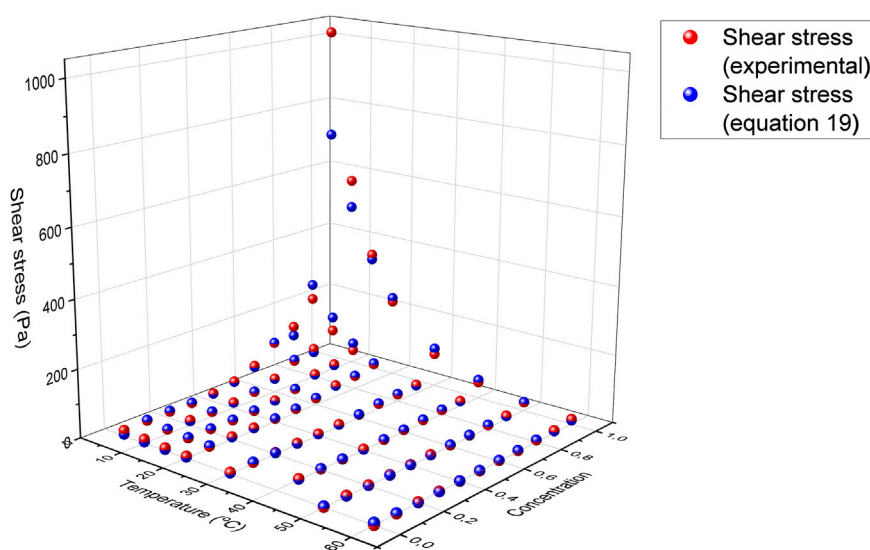


FIGURE 9 Comparison of experimental and model-calculated shear stress values for binary crude oil mixtures at a constant shear rate.

Vankor crude exhibited a nearly linear relationship between shear stress and shear rate, indicating Newtonian behavior across the studied temperature range.

The dynamic viscosity of the mixtures decreased monotonically with increasing temperature and with increasing fraction of the low-viscosity component. The most significant reduction in viscosity occurred within the temperature range of 20 °C–40 °C, corresponding to the phase transition from a structured dispersed system to a predominantly homogeneous liquid phase. At temperatures above 40 °C, the viscosity–temperature curves became less steep, indicating the attenuation of intermolecular associations.

## 5.1 Validation and performance analysis of the proposed rheological model

After determining the main parameters  $K$  and  $n$ , the shear stress was calculated at a constant shear rate using the proposed rheological model. The obtained values were plotted together with the experimental data for comparison. The resulting graph, presented in Figure 9, demonstrates a close agreement between the experimental and calculated shear stress values, confirming the validity of the proposed model under the studied conditions.

The results obtained for the shear stress at different temperatures and concentrations of heavy crude oil are summarized in Table 4. The third column presents experimentally measured values, while the fourth column corresponds to those calculated using the proposed rheological model.

A quantitative comparison between the experimental and model-predicted shear stress values demonstrates a high level of agreement. The relative deviation  $\delta$  between experimental  $\tau_{\text{exp}}$  and calculated  $\tau_{\text{calc}}$  values was evaluated using the expression as Equation 23

$$\delta = \frac{|\tau_{\text{exp}} - \tau_{\text{calc}}|}{\tau_{\text{exp}}} \cdot 100\% \quad (23)$$

The mean relative deviation across all data points did not exceed 8.7%, while the root mean square error (RMSE) was less than 0.95 Pa, which indicates excellent predictive accuracy for practical engineering applications.

In addition to global performance metrics, the distribution of relative deviations was analyzed. The residuals exhibited an approximately symmetric distribution centered near zero, indicating the absence of systematic bias across the investigated operating conditions.

Assuming a normal distribution of residuals, a 95% confidence interval for the predicted shear stress was estimated based on the RMSE. For most temperatures and mixture compositions, the confidence bounds remained within  $\pm 1.9$  Pa, confirming the statistical stability of the model predictions.

A comparison of the data demonstrates that the model reproduces the experimental results with high accuracy across the entire range of studied temperatures (5 °C–60 °C) and concentrations (0–1). The deviations between the experimental and calculated shear stress values do not exceed 10%–12% for most conditions, confirming the reliability of the adopted parameterization and the physical adequacy of the model.

At higher temperatures (50 °C–60 °C), the experimental and calculated curves nearly coincide, indicating that the model correctly captures the transition of the mixture toward Newtonian flow. In this temperature region, the weakening of molecular interactions leads to reduced structural viscosity, and the flow behavior index  $n$  approaches unity.

A systematic analysis of prediction errors indicates that the largest deviations occur at temperatures below 15 °C and heavy crude concentrations exceeding 0.7. These conditions represent the boundary of the validated applicability range, where strong structural heterogeneities and time-dependent effects become

TABLE 4 Comparison of experimental and model-calculated shear stress values at different temperatures and concentrations of heavy crude oil.

T, °C	C	$\tau$ exp, Pa	$\tau$ calc, Pa	T, °C	C	$\tau$ exp, Pa	$\tau$ calc, Pa	T, °C	C	$\tau$ exp, Pa	$\tau$ calc, Pa
60	0,1	1,26	6,92	40	0,8	12,94	13,66	15	0,5	17,68	17,64
60	0,2	1,58	1,61	40	0,9	14,96	14,49	15	0,6	28,28	28,33
60	0,3	1,32	1,31	40	1	48,14	55,29	15	0,7	49,90	49,06
60	0,4	1,12	1,11	30	0	3,97	3,36	15	0,8	57,42	54,74
60	0,5	1,25	1,26	30	0,1	4,49	4,62	15	0,9	78,87	100,87
60	0,6	1,58	1,58	30	0,2	4,33	4,33	15	1	360,58	345,83
60	0,7	2,32	2,33	30	0,3	4,19	4,16	10	0	11,74	3,84
60	0,8	3,28	3,31	30	0,4	4,70	4,66	10	0,1	14,40	14,82
60	0,9	6,42	6,62	30	0,5	6,36	6,26	10	0,2	14,30	13,08
60	1	8,15	6,44	30	0,6	10,14	10,14	10	0,3	14,27	14,67
60	0	15,22	12,50	30	0,7	17,20	18,21	10	0,4	16,95	16,69
50	0,1	1,54	2,65	30	0,8	21,18	22,33	10	0,5	25,09	25,36
50	0,2	2,10	2,09	30	0,9	26,02	24,09	10	0,6	41,26	40,75
50	0,3	1,74	1,73	30	1	98,51	115,68	10	0,7	73,78	76,31
50	0,4	1,64	1,64	20	0	5,97	3,49	10	0,8	87,72	77,32
50	0,5	1,85	1,85	20	0,1	7,30	8,51	10	0,9	124,43	165,77
50	0,6	2,73	2,71	20	0,2	7,37	7,34	10	1	577,42	495,71
50	0,7	3,47	3,48	20	0,3	7,27	7,23	5	0	17,13	5,01
50	0,8	5,25	5,25	20	0,4	8,51	8,52	5	0,1	20,13	20,54
50	0,9	8,70	9,13	20	0,5	12,39	12,48	5	0,2	20,62	22,01
50	1	10,20	9,81	20	0,6	20,04	20,30	5	0,3	20,99	21,25
50	0	25,76	26,32	20	0,7	34,23	33,61	5	0,4	24,91	24,82
50	0,1	2,31	2,65	20	0,8	39,57	39,86	5	0,5	37,40	36,45
40	0,2	2,90	2,85	20	0,9	52,37	55,92	5	0,6	62,37	59,07
40	0,3	2,61	2,62	20	1	229,29	240,58	5	0,7	111,40	112,38
40	0,4	2,31	2,31	15	0	8,28	3,66	5	0,8	140,82	113,00
40	0,5	2,94	2,87	15	0,1	10,02	11,10	5	0,9	208,73	252,91
40	0,6	3,68	3,71	15	0,2	10,11	10,43				
40	0,7	5,74	5,76	15	0,3	9,88	10,08				

increasingly significant. In this regime, the relative deviation increases due to the enhanced contribution of temperature-sensitive structural phenomena, such as asphaltene aggregation and paraffin crystallization.

The increased deviations observed at temperatures below approximately 15 °C can be attributed to physicochemical phenomena that are only partially captured by the steady-state power-law framework. At low temperatures, heavy crude oil mixtures exhibit enhanced structural heterogeneity due to intensified asphaltene aggregation, paraffin crystallization, and the formation of transient network structures. These processes introduce time-dependent and history-dependent rheological effects, including thixotropy and weak viscoelasticity, which are not explicitly represented in the present formulation.

In addition, low-temperature conditions amplify the sensitivity of rheological properties to minor compositional fluctuations and experimental uncertainties, particularly at high heavy-oil concentrations. As a result, localized deviations between experimental and predicted shear stress values become more pronounced. Future extensions of the model may incorporate structural kinetics, viscoelastic constitutive terms, or temperature-dependent yield stress formulations to better capture these effects. Nevertheless, within the validated temperature and concentration range, the current model provides stable and physically consistent predictions suitable for engineering calculations.

The dependence of shear stress on concentration at a constant shear rate (Figure 4) shows a clearly nonlinear character. At low

TABLE 5 Comparison of predictive accuracy of different models.

Model	Temperature dependence	Concentration dependence	Non-newtonian behavior	Mean relative deviation, %
Arrhenius	Yes	No	No	22–28
Refutas	No	Yes	No	18–24
Classical power-law	No	No	Yes	15–20
Proposed model	Yes	Yes	Yes	8.7

concentrations ( $C < 0.4$ ), the addition of a light component causes a rapid decrease in shear stress—a typical dilution effect. However, at higher concentrations ( $C > 0.7$ ), the effect becomes weaker, and the mixture behaves similarly to a structured non-Newtonian fluid. The experimental and model-predicted surfaces coincide closely, confirming that the proposed Equations 8–10 adequately describe the joint influence of thermal and compositional factors on the rheological properties of binary crude oil mixtures.

Overall, the results validate the applicability of the developed model for predicting shear stress and viscosity under a wide range of operating conditions. The high level of agreement between experimental and calculated data demonstrates that the inclusion of inter-component interaction coefficients significantly improves the accuracy of rheological predictions compared with classical models.

A qualitative sensitivity assessment indicates that model predictions at low temperatures are primarily governed by the consistency coefficient parameters, whereas at higher temperatures and lower heavy oil concentrations, the flow behavior index becomes the dominant factor.

## 5.2 Comparison with established rheological models

To demonstrate the practical use of the proposed rheological model, its predictions for the same experimental conditions were directly compared with those obtained using widely adopted Arrhenius, Refutas, and classical power-law models.

To quantitatively assess the performance of the proposed rheological model, its predictive accuracy was compared with several widely used viscosity and rheological correlations reported in the literature. Specifically, the Arrhenius temperature–viscosity model, the Refutas viscosity blending rule, and the classical power-law model with constant parameters were applied to the same experimental dataset.

All reference models were calibrated using the same experimental data and evaluated under identical temperature and concentration conditions to ensure a fair comparison (Table 5). The comparison is performed using the same temperature, composition, and shear rate conditions as those employed in the validation example presented in Figure 9 and Table 4.

The comparison demonstrates that conventional viscosity correlations exhibit substantially higher prediction errors when applied to non-Newtonian crude oil mixtures under varying temperature and compositional conditions. Models accounting for only one governing factor—temperature, concentration, or shear

dependence—fail to reproduce the coupled effects observed experimentally.

In contrast, the proposed model explicitly incorporates temperature-dependent non-Newtonian behavior and inter-component interactions, resulting in a significantly lower prediction error across the entire operating domain. This confirms the practical advantage of the model for pipeline transport applications in cold climate conditions.

The superior predictive performance of the proposed model is consistent with the qualitative sensitivity trends discussed above, further confirming its robustness across the investigated operating conditions.

## 6 Conclusion

In this study, a physically based rheological model was developed to describe the flow behavior of non-Newtonian crude oil mixtures under cold climate conditions. The model incorporates temperature- and concentration-dependent expressions for the consistency coefficient and flow behavior index, introducing inter-component interaction coefficients to account for nonlinear blending effects.

Experimental investigations using high-viscosity crude from the Severo-Komsomolskoye field and low-viscosity crude from the Vankor field were performed over a temperature range of 5 °C–60 °C. The obtained results demonstrated strong agreement between experimental and calculated shear stress values, with a mean relative deviation of less than 8.7% and a root mean square error below 0.95 Pa.

The model successfully reproduces the transition from non-Newtonian to Newtonian flow regimes as temperature increases or as the mixture becomes more diluted. It accurately predicts the nonlinear variation of viscosity and shear stress with both temperature and concentration.

The developed model provides a reliable tool for optimizing pipeline transport of heavy crudes, improving flow assurance, and reducing energy consumption in cold environments. Future research will extend the model to multiphase systems and include viscoelastic effects for more complex crude compositions.

Future research will focus on extending the proposed rheological framework to a broader range of crude oil systems and operating conditions. In particular, the model may be adapted to multiphase oil–water mixtures, emulsified systems, and crude oils containing higher wax or asphaltene contents. Incorporation of viscoelastic and thixotropic constitutive elements would further improve prediction accuracy under transient flow conditions, such as start-up, shutdown, and flow rate fluctuations.

In addition, coupling the proposed rheological model with hydraulic and thermal pipeline simulators would enable integrated

flow assurance analysis under spatially varying temperature fields. The model may also be extended to account for pressure effects and chemical additives, providing a unified framework for evaluating dilution, heating, and drag-reduction strategies. These developments would broaden the applicability of the proposed approach and support its use in advanced pipeline design and operational optimization for complex and cold-region environments.

## Data availability statement

The raw data supporting the conclusions of this article will be made available by the authors, without undue reservation.

## Author contributions

AN: Methodology, Supervision, Writing – review and editing. AG: Writing – original draft, Visualization, Data curation. KP: Writing – original draft, Conceptualization, Formal Analysis.

## Funding

The author(s) declared that financial support was not received for this work and/or its publication.

## References

- Al-Basrah, A. S. (2004). New method for predicting the viscosity of oil blends. *Energy and Fuels* 18, 1414–1419.
- Al-Maamari, R. S., Vakili-Nezhaada, G., and Vatani, M. (2015). Experimental and modeling investigations of the viscosity of crude oil binary blends: new models based on the genetic algorithm method. *J. Eng. Res. [TJER]* 12 (1), 81. doi:10.24200/tjer.vol12iss1pp81-91
- Buslaev, G. V., and Konoplyannikov, A. V. (2026). Mathematical modeling of a hydro-mechanical system with a positive displacement motor and hydraulic thruster to optimize the drilling process for extended-reach drilling Wells. *Int. J. Eng.* 39 (5), 1077–1087. doi:10.5829/ije.2026.39.05b.03
- Chevron Research Company. (1979). Chevron viscosity blending chart.
- Cragoe, C. S. (1929). *Techniques for the prediction of physical properties of petroleum fractions*. Washington, DC: Bureau of Standards Journal.
- Dvoynikov, M. V., and Kutuzov, P. A. (2025). Analysis of efficiency of communication channels for monitoring and operational control of oil and gas Wells drilling process. *Int. J. Eng.* 38 (1), 120–131. doi:10.5829/ije.2025.38.01a.12
- Falconi, M., Tamayo, E., Laurencio, H., Vega, J., Gualotuña, E., Edwin, R. G., et al. (2018). Model of pressure losses in pipes during the transport of heavy oil with 11 API gravity.
- Gudala, M., Naiya, T., and Govindarajan, S. (2020). Remediation of heavy oil transportation problems via pipelines using biodegradable additives: an experimental and artificial intelligence approach. *Spe J.* 26, 1050–1071. doi:10.2118/203824-PA
- Hoshyargar, V., and Ashrafizadeh, S. (2013). Optimization of flow parameters of heavy crude oil-in-water emulsions through pipelines. *Industrial and Eng. Chem. Res.* 52, 1600–1611. doi:10.1021/IE302993M
- Huan, X., Jagalur, J., and Marzouk, Y. (2024). Optimal experimental design: formulations and computations. *Acta Numer.* 33, 715–840. doi:10.1017/S0962492924000023
- Jackson, M. (1994). Optimal design of experiments. *J. Operational Res. Soc.* doi:10.5860/choice.31-0986
- Jing, J., Yin, R., Yuan, Y., Shi, Y., Sun, J., and Zhang, M. (2020). Determination of the transportation limits of heavy crude oil using three combined methods of heating, water blending, and dilution. *ACS Omega* 5, 9870–9884. doi:10.1021/acsoomega.0c00097
- Jing, J., Guo, Y., Karimov, R., Sun, J., Huang, W., Chen, Y., et al. (2023). Drag reduction related to boundary layer control in transportation of heavy crude oil by

## Conflict of interest

The author(s) declared that this work was conducted in the absence of any commercial or financial relationships that could be construed as a potential conflict of interest.

## Generative AI statement

The author(s) declared that generative AI was not used in the creation of this manuscript.

Any alternative text (alt text) provided alongside figures in this article has been generated by Frontiers with the support of artificial intelligence and reasonable efforts have been made to ensure accuracy, including review by the authors wherever possible. If you identify any issues, please contact us.

## Publisher's note

All claims expressed in this article are solely those of the authors and do not necessarily represent those of their affiliated organizations, or those of the publisher, the editors and the reviewers. Any product that may be evaluated in this article, or claim that may be made by its manufacturer, is not guaranteed or endorsed by the publisher.

pipeline: a review. *Industrial and Eng. Chem. Res.* 62, 14818–14834. doi:10.1021/acs.iecr.3c02212

Kendall, J., and Monroe, K. P. (1917). The viscosity of liquids. *Industrial Eng. Chem.* 9, 357–359.

Koval, E. J. (1963). A method for predicting the performance of unstable miscible displacement in heterogeneous media. *SPE J.* 3, 145–154. doi:10.2118/450-PA

Kumar, S., and Mahto, V. (2017). Emulsification of Indian heavy crude oil using a novel surfactant for pipeline transportation. *Petroleum Sci.* 14, 372–382. doi:10.1007/s12182-017-0153-6

Litvinenko, V. S., Tsvetkov, P. S., Dvoynikov, M. V., and Buslaev, G. V. (2020). Barriers to implementation of hydrogen initiatives in the context of global energy sustainable development. *J. Min. Inst.* 244, 428–438. doi:10.31897/PMI.2020.4.5

Lyu, S., He, Y., Yao, Y., Zhang, M., and Wang, Y. (2019). Photothermal clothing for thermally preserving pipeline transportation of crude oil. *Adv. Funct. Mater.* 29, 1900703. doi:10.1002/adfm.201900703

Maxwell, J. C. (1972). *Petroleum engineer handbook*. Houston, TX: Gulf Publishing.

Mehrotra, A. K., Monnery, W. D., and Svrcek, W. Y. (1996). A review of practical calculation methods for the viscosity of liquid hydrocarbons and their mixtures. *Fluid Ph. Equilib.* 117 (1–2), 344–355. doi:10.1016/0378-3812(95)02971-0

Miadonye, A., Latour, N., and Puttagunta, V. R. (2000). A correlation for viscosity and solvent mass fraction of bitumen-diluent mixtures. *Petrol. Sci. Technol.* 18 (1–2), 1–14. doi:10.1080/10916460008949828

Parkash, S. (2003). *Refining processes handbook*. Houston, TX: Gulf Publishing Company.

Pilehvari, A., Saadevandi, B., Halvaci, M., and Clark, P. (1988). Oil/water emulsions for pipeline transport of viscous crude oils. *Softw. - Pract. Exp.* doi:10.2118/18218-MS

Pshenin, V., Sleptsov, A., and Dukhnevich, L. (2025). Prospects of improving the vibroacoustic method for locating buried non-metallic pipelines. *Eng* 6 (6), 121. doi:10.3390/eng6060121

Refutas, L. (1991). Calculations of viscosities of mixtures and blends using viscosity blending numbers. *Hydrocarb. Process.* 70, 114–116.

Riazi, M. R. (2005). Characterization and properties of petroleum fractions.

Robidas, B., and Gogoi, S. (2020). Effects of temperature on the transportation of Assam crude oil through pipelines. 259–273. doi:10.1201/9781003049937-15

Rushd, S., Ferroudji, H., Yousuf, H., Walker, T., Basu, A., and Sen, T. (2023). Applications of drag reducers for the pipeline transportation of heavy crude oils: a critical review and future research directions. *Can. J. Chem. Eng.* 102, 438–458. doi:10.1002/cjce.25023

Saleh, S., Mohammed, T., Hassan, H., and Barghi, S. (2021). CFD investigation on characteristics of heavy crude oil flow through a horizontal pipe. *Egypt. J. Petroleum* 30, 13–19. doi:10.1016/j.ejpe.2021.06.003

Shamzov, I. A., Borisov, A. V., Aleksandruk, B. S., Lopatenko, G. V., and Nikitina, V. (2025). Algorithmic models for determining the flow patterns of oil pipelines in gravity sections. *Int. J. Eng. Trans. A Basics*. 38 (10), 2476–2485. doi:10.5829/ije.2025.38.10a.22

Shan, Z., and Peng, Y. (2004). A model for viscosity estimation of multicomponent hydrocarbon mixtures. *J. Petroleum Sci. Eng.* 42, 25–34.

Silva-Oliver, G., Ramírez-Jiménez, E., Sánchez-Minero, F., Valdés-Pastrana, H., Méndez, F., Ascanio, G., et al. (2020). Theoretical evaluation of dilution processes

versus thermal effects induced on the transport of heavy oil. *J. Petroleum Sci. Eng.* 192, 107246. doi:10.1016/j.petrol.2020.107246

Skorobogatov, A. A., Pshenin, V. V., Tsvetkova, C. P., and Borisov, R. A. (2025). Multiphase oil-water flow in horizontal and inclined pipelines. Effect of flow velocity on flow patterns. *Int. J. Eng.* 38 (8), 1820–1830. doi:10.5829/ije.2025.38.08b.08

Souas, F., Safri, A., and Benmounah, A. (2020). A review on the rheology of heavy crude oil for pipeline transportation. *Petroleum Res.* 6, 116–136. doi:10.1016/j.ptlrs.2020.11.001

Wallace, J. S., and Henry, F. J. (1955). Empirical correlation of oil blend viscosity. *Pet. Refin.*

Walter, D. H. (1951). The effect of temperature on the viscosity of oil mixtures. *Fuel.*